On the Regulation of the Pacific Warm Pool Temperature

Ming-Dah Chou[1], Sue-Hsien Chou[1], and Pui-King Chan[2]

Popular Summary

Submitted to Journal of Climate

The water temperature of the tropical western Pacific (Pacific warm pool) is very high but rarely greater than 30°C. It is very important to understand the processes that prevent the temperature from increasing to a value higher than 30°C. Scientists have proposed a number of hypotheses that regulate the warm pool temperature. These hypotheses include the reduction of solar heating due to clouds, the enhanced evaporative cooling due to warm water, and the efficiency of winds in transporting heat.

By analyzing the surface wind, clouds, and heat fluxes in the warm pool, we have found that regions of the highest sea surface temperature have the largest surface heating. It is clear that an enhanced heating in the warmest region is not sustainable and must be interrupted by variations in large-scale atmospheric circulation. As the deep convective regions shift away from high temperature regions due to seasonal variation of the atmospheric circulation, both wind and evaporative cooling in the warm regions increase, leading to a reduction in temperature. We conclude that the evaporative cooling associated with the seasonal variation of wind is the primary factor that prevents the warm pool temperature from increasing to a value much higher than 30°C.

[1]Laboratory for Atmospheres, NASA Goddard Space Flight Center, Greenbelt, MD 20771

[2]Pui-King Chan, Science Systems & Applications, Inc., Lanham, MD 20706

On the Regulation of the Pacific Warm Pool Temperature

Ming-Dah Chou, Shu-Hsien Chou
Laboratory for Atmospheres
NASA Goddard Space Flight Center
Greenbelt, MD 20771

Pui-King Chan
Science Systems & Applications, Inc.
Lanham, MD 20706

September 2002
To be submitted to Journal of Climate

Corresponding author address: Dr. Ming-Dah Chou
Code 913
NASA/Goddard Space Flight Center
Greenbelt, MD 20771
Telephone: 301-614-6192
Fax: 301-614-6307
Email: chou@climate.gsfc.nasa.gov

Abstract

In the tropical western Pacific, regions of the highest sea surface temperature (SST) and the largest cloud cover are found to have the largest surface heating, primarily due to the weak evaporative cooling associated with weak winds. This situation is in variance with the suggestions that the temperature in the Pacific warm pool is regulated either by the reduced solar heating due to an enhanced cloudiness or by the enhanced evaporative cooling due to an elevated SST. It is clear that an enhanced surface heating in an enhanced convection region is not sustainable and must be interrupted by variations in large-scale atmospheric circulation. As the deep convective regions shift away from regions of high SST due primarily to seasonal variation and secondarily to interannual variation of the large-scale atmospheric and oceanic circulation, both trade wind and evaporative cooling in the high SST region increase, leading to a reduction in SST. We conclude that the evaporative cooling associated with the seasonal and interannual variations of trade winds is the primary factor that prevent the warm pool SST from increasing to a value much higher than what is observed.

1. Introduction

The tropical western Pacific is warm and cloudy. The sea surface temperature between 20°S and 20°N is nearly homogeneous with a magnitude between 28°C and 30°C. Regions with SST>30°C are rare and are association with a stable and clear atmosphere with descending air (Waliser and Graham, 1993). Ramanathan and Collins (1991) hypothesized that the increase in thick cirrus clouds in response to an increase in SST had an effect of reducing the solar heating of the ocean and limit the SST to the observed high values. Subsequently, various mechanisms were proposed by a number of investigators that regulate the SST in the Pacific warm pool (e.g. Fu et al. 1992; Hartmann and Michelsen, 1993; Lau et al. 1994; Pierrehumbert, 1995; Stephens and Slingo, 1992; Sud et al. 1999; Wallace, 1992). Most of those studies stressed the importance of large-scale circulation in distributing heat. Some also stressed the importance of the high sensitivity of evaporation to high temperature in regulating the SST. In addition to the magnitude of SST, a relevant question also can be raised as to the mechanisms that cause the SST in the warm pool homogeneous. Wallace (1992) reasoned that the homogeneous tropospheric temperature in the tropics is a result of the efficient heat transport by large-scale circulation. Because of the high sensitivity of evaporation to SST in the warm pool, the difference between the air and sea temperatures is necessarily small, and so is the SST gradient. In addition to viewing the issue from the large-scale aspect, analysis of the surface heat budgets can also provide information on the causes that lead to a homogeneous SST distribution in the Pacific warm pool. We have derived from satellite radiance measurements complete sets of surface heat fluxes of the tropical western Pacific covering the period October 1997–December 2000. In this note, we use these data sets of surface heating to investigate the mechanisms that regulate the SST of the Pacific warm pool.

2. Data source

The data used in this study include the SST, surface wind, high-level clouds, and the surface radiative and turbulent heat fluxes. All the data have a spatial resolution of 1°x1° latitude-longitude and a temporal resolution of 1 day except for the SST, which has a temporal resolution of 1 week. The SST is taken from the National Centers for Environmental Prediction (NCEP) archive (Reynolds and Smith, 1994), and the surface wind is taken from the Special Sensor Microwave Imager (SSM/I) wind retrieval (Wentz, 1997). The high-level cloud cover is inferred from the brightness temperature measured in the 11-μm channel of Japan's Geostationary Meteorological Satellite-5 (GMS-5) using a threshold temperature of 260 K. The GMS pixels have a spatial resolution of 5-km and a temporal resolution of 1 hr. The high-level cloud cover is inferred at these high spatial and temporal resolutions and then averaged to a spatial resolution of 1°x1° latitude-longitude and a temporal resolution of 1 day (Chou et al. 2001).

The surface latent and sensible heat fluxes are derived from the improved algorithms of Chou et al. (1997), which use the NCEP SST analysis and the SSM/I precipitable water and wind retrievals (Wentz, 1997). The derived latent and sensible heat fluxes have been validated against the measurements onboard research ships in five tropical field experiments (Chou et al. 2002). The surface solar and IR radiative fluxes are empirically derived from the GMS-5 measurements of the albedo in the 0.6-μm channel and the brightness temperature in the 11-μm channel, respectively. The inferred surface solar and IR fluxes have been validated against the measurements at the US Department of Energy's Atmospheric Radiation Measurement site on Manus island in the western equatorial Pacific (Chou et al. 2001).

The surface latent and sensible heat fluxes cover the period July 1987–December 2000, and the surface solar and thermal infrared fluxes cover the period October 1997–December 2000. The turbulent and radiative fluxes are available, respectively, at the ftp sites

http://daac.gsfc.nasa.gov/CAMPAIGN_DOCS/hydrology/hd_gsstf2.0.html

and http://daac.gsfc.nasa.gov/CAMPAIGN_DOCS/hydrology/hd_gssrb.html

3. Seasonal and interannual variations

In the tropical western Pacific, the sea surface temperature is high. It is in the ascending branch of both the Hadley and Walker circulations. Trade winds converge in this region that induce strong deep convection and produce large amount of clouds. Figure 1 shows the SST, high-level cloud cover, and wind speed averaged over a three-year period January 1998–December 2000. Regions of high sea surface temperature cover most of the western Pacific and eastern Indian Oceans in the tropics (20°S-20°N). These high SST regions have a high cloud cover (middle panel) and small wind speed (lower panel). Clouds reflect the incoming solar radiation and reduce the solar heating of the ocean. On the other hand, weak winds cause a weak evaporative cooling. Figures 2 shows the net downward solar flux, latent heat flux, and the total heat (solar, infrared, latent heat and sensible heat) flux at the sea surface averaged over the same three-year period. As can be seen from Figs. 1 and 2, the distribution of the surface solar heating follows that of clouds, and the distribution of evaporative cooling follows that of surface winds. The magnitude of the solar heating is significantly larger than that of the evaporative cooling, but the spatial variation is larger for the latter (~90 W m^{-2}) than for the former (~50 W m^{-2}). As a result, the spatial distribution of the total surface heating follows that of the evaporative cooling (middle and lower panels of Fig. 2). Because the spatial variation of evaporative cooling is larger than that of solar heating, regions of the maximum total surface heating are regions of maximum cloud cover and minimum wind speed. Data from the NCEP/National Center for Atmospheric Research reanalysis (Kalnay et al. 1996) for the same three-year period also show the same results that the maximum surface heating coincides with the maximum cloud cover due to the reduced evaporative cooling. The reduced evaporative cooling in the convective regions was also shown by Ramanathan and Collins (1992).

It is noted that there is a significant amount of solar radiation penetrating through the bottom of the ocean mixed layer. In the warm pool region, it amounts to ~35 W m^{-2} during the Tropical Ocean and Global Atmosphere, Coupled Ocean-Atmosphere Response Experiment

(TOGA COARE) period November 1992–February 1993 (Chou et al. 2000). This amount of solar radiation is not available for heating the ocean mixed layer.

The maximum surface heating in the high SST and strong convective region is in variance with the cirrus-cloud thermostat hypothesis of Ramanathan and Collins (1991) that an increase in the cloud cover leads to a reduction in the solar heating and SST. It is also in variance with the suggestion by Wallace (1992) that the evaporative cooling would increase with increasing SST and, hence, imposed an upper limit to the SST. With the maximum heating occurring at high SST regions, one might wonder what are the physical mechanisms that would prevent the SST from increasing further. The answer lies on the transient nature of the solar radiation and the atmospheric circulation. The surface heating and cooling shown in Figure 2 are for an annual mean over three years (1998-2000). Due to the seasonal variations of the insolation at the top of the atmosphere and the corresponding shifts in the intertropical convergence zone (ITCZ) and trade winds, the maximum heating as shown in the lower panel of Figure 2 does not occur in all seasons.

For a given season, generally the regions of maximum cloudiness, i.e. ITCZ, follow the maximum SST, minimum winds, and maximum insolation at the TOA. As the season advances, the Sun moves away from this maximum SST region to the neighboring regions where are less cloudy. The neighboring regions then receive much solar heating, the SST increases, the convergence zone follows, and the wind speed decreases. The decrease in wind speed further enhances SST and convection in the neighboring regions. Simultaneously, the region of maximum surface heating in the previous season experiences a decrease in clouds and an increase in winds, which enhances the evaporative cooling. The high SST region in the previous season is then cools down as the Sun moves away and the strong trade winds set in.

The processes outlined above can be demonstrated in Fig. 3, which shows time series of the SST, the insolation at the top of the atmosphere (S_o), the surface solar heating (SW), and the evaporative cooling (LH) averaged over the warmest region of the Pacific (5° N-15° N, 130° E-

160° E). The insolation reaches a minimum in December and increases till April. It remains nearly constant from April through September and decreases afterward as the Sun moves southward. From April to September, S_o remains nearly constant, but SW decreases, indicating an increase in cloudiness. Simultaneously, LH also decreases but with a much larger rate than SW, indicating a much reduced wind speed in the convective and high cloudiness region. After August-September, the Sun moves southward, the SW keeps decreasing, but the evaporative cooling enhances when the strong northeast trade wind sets into this region. The SST follows S_o with a lag of ~2 months.

Figure 4 shows differences in the SST, the cloud cover, and the surface wind speed between the months of December, January, and February (DJF) and the months of June, July, and August (JJA). Following the position of the Sun, the SST increases in the summer and decreases in the winter. The ITCZ moves from the Northern Hemisphere in JJA to the Southern Hemisphere in DJF. Consistent with the position of the ITCZ, the strong southeast trade wind south of the equator during JJA is replaced by converging weak winds during DJF. Similarly, the weak wind north of the equator during JJA is replaced by the strong northeast trade wind during DJF. Responses of the surface heating to the seasonal changes in SST, clouds and winds are shown in Fig. 5. In spite of a larger cloudiness, the surface solar heating increases from to JJA to DJF in the Southern Hemisphere due to an increase in the TOA insolation, whereas the evaporative cooling decreases due to a reduced wind speed. The results is a large increase in the total surface heating, by ~100 W m^{-2} at 10°S latitude. This large surface heating and the associated increase in SST is not sustainable over a period of a season because the Sun and the ITCZ will soon move away from this maximum heating region.

Regulation of the warm pool SST by the large-scale circulation can also be demonstrated using the data pertaining to interannual variations. A strong El Nino occurred in 1997 when the central and eastern Pacific was anomaly warm. The SST changed to a new La Nina phase in May 1998. Figure 6 shows the differences in SST, fractional cloud cover, and wind speed between the

NH winters (December, January, February; DJF) of 1997-1998 and 1998-1999. The central equatorial region warmed significantly by > 2°C during the 1997-1998 El Nino. Following the shift in SST, the convective zone, which is normally located in the maritime continent, shifted eastward by ~ 60° longitude. Cloud cover increased, and wind speed decreased significantly in the central equatorial Pacific. The corresponding changes in the surface heating are shown in Fig. 7. Compared to DJF of 1998-1999, both the surface solar heating and evaporative cooling in the central equatorial Pacific decrease during the El Nino. Dominated by the decrease in wind speed and evaporative cooling, the total heating increased by ~30 W m^{-2} regardless of the decrease in solar heating. The anomalous SST and wind in the central equatorial Pacific gradually entered into a La Nina after April 1998 due to oscillations in atmospheric and oceanic circulation.

4. Concluding remarks

Analysis of data on clouds, winds, and surface heat fluxes shows that the transient behavior of basin-wide large-scale circulation is the major mechanism that limits the warm pool SST to the observed maximum value Neither the reduction in the solar heating in response to increasing cloudiness nor the enhanced sensitivity of evaporative cooling to increasing SST is the mechanism that regulates warm pool SST.

Trade winds converge to regions of the highest SST in the equatorial western Pacific. These regions have the largest cloud cover and smallest wind speed. Both surface solar heating and evaporative cooling are weak. The spatial variation of evaporative cooling is significantly larger than that of solar heating, and the distribution of the total surface heating is found to follow the distribution of the evaporative cooling, which have a minimum in the strong convective and high SST regions. The result is a maximum heating in the strong convective and high SST regions. This is in variance with the suggestions by previous studies that either high cloud cover or strong evaporation reduces the surface heating in warm and cloudy regions.

It is obvious that the situation in which the largest surface heating occurs in the warmest regions is not sustainable Due to the seasonal variation of the insolation at the top of the atmosphere, trade winds and clouds also experience seasonal variations. As the Sun moves away from a convective region, the strong trade winds set in, and the evaporative cooling enhances, resulting in a net cooling of the surface. Therefore, the SST is primarily regulated by evaporative cooling associated with strong trade winds. During an El Nino, the maximum SST and convective region shifts eastward from the maritime continent by 60° longitude to the equatorial central Pacific. Following the eastward shift of the maximum SST, the region of maximum cloudiness and surface heating also shifted eastward. As the atmospheric and oceanic circulation returns to normal situations, the trade winds increase and the surface heating decreases.

It would be interesting to ask the hypothetical questions as to how much higher the SST can go and how much the SST gradient can change if there were no seasonal variations in the insolation and the large-scale circulation. These questions are relevant to the suggestion by Wallace (1992) that the tropical SST is regulated by the efficient transport of heat in the atmosphere and the high sensitivity of evaporation to SST. Perhaps these questions can only be answered with reliable climate simulations using a coupled atmosphere-ocean model.

As suggested by Pierrehumbert (1995), neither evaporation nor clouds can serve as a major thermostat for the tropical climate. The tropical climate is determined by complicated interactions between the large-scale circulation, the radiative heating, and the evaporative cooling. In this note we address only the cause that prohibits the warm pool SST from increasing to a value much higher than the observed value. We have not addressed the processes that regulate the tropical climate as a whole.

Acknowledgments This work was supported by the TRMM Program, Global Modeling and Analysis Program, and Radiation Research Program, NASA/Office of Earth Science. The wind data were provided by F. Wentz through the website http://www.ssmi.com. The SST data were obtained from the NCEP/NCAR reanalysis. The GMS albedoe and brightness temperature archived at the Central Weather Bureau, Taiwan, were provided by Kung-Hwa Wang of the Taiwanes Central Weather Bureau. Daily GSSTF-2 air-sea turbulent fluxes were processed by E. Nelkin and J. Ardizzone.

References

Chou, M.-D., P.-K. Chan, and M. M.-H. Yan 2001: A sea surface radiation data set for climate applications in the tropical western Pacific and South China Sea. *J. Geophy. Res.*, ***106***, 7219-7228.

Chou, S.-H., C.-L. Shie, R. M. Atlas, and J. Ardizzone, 1997: Air-sea fluxes retrieved from Special Sensor Microwave Imager data. *J. Geophys. Res.*, **102**, 12705-12726.

Chou, S.-H., W. Zhao, and M.-D. Chou, 2000: Surface Heat Budgets and Sea Surface Temperature in the Pacific Warm Pool During TOGA COARE, *J. Climate*, **13**, 634-649.

Chou, S.-H., M.-D. Chou, P.-K. Chan, and P.-H. Lin 2002: Surface Heat Budgets and Sea Surface Temperature in the tropical western Pacific and the eastern Indian ocean. *J. Climate,* to be submitted.

Fu, R., A. D. Del Genio, W. B. Rossow, and W. T. Liu, 1992: Cirrus-cloud thermostat for tropical sea surface temperatures tested using satellite data. *Nature*, **358**, 394-397.

Hartmann, D. L., and M. L. Michelsen, 1993: Large-scale effects on the regulation of tropical sea surface temperature. *J. Climate*, **6**, 2049-2062.

Kalnay, E., M. Kanamitsu, R. Kistler, W. Collins, D. Deaven, L. Gandin, M. Iredell, S. Saha, G. White, J. Woollen, Y. Zhu, M. Chelliah, W. Ebisuzake, W. Higgins, J. Janowiak, K. C. Mo., C. Ropelewski, J. Wang, A. Leetmaa, R. Reynolds, R. Jenne, and D. Joseph, 1996: The NCEP/NCAR 40-year reanalysis project. *Bull. Amer. Meteorol. Soc.*, **77**, 437-471.

Lau, K.-M., C.-H. Sui, M.-D. Chou and W.-K. Tao, 1994: An inquiry into the cirrus-cloud thermostat effect for tropical sea surface temperature. *Geophy. Res. Letter*, **21**, 1157-1160.

Pierrehumbert, R. T., 1995: Thermostats, radiator fins, and the local runaway greenhouse. *J. Atmos. Sci.*, **52**, 1784-1806.

Ramanathan, V., and W. Collins, 1991: Thermodynamic regulation of ocean warming by cirrus clouds deduced from observations of the 1987 El Nino. *Nature*, **351**, 27-32.

Ramanathan, V., and W. Collins, 1992: Thermostat and global warming. *Nature*, **357**, 649-649.

Reynolds, R. W. and T. M. Smith, 1994: Improved global sea surface temperature analyses. *J. Climate, 7,* 929-948.

Stephens, G. L., and A. Slingo, 1992: An air-conditioned greenhouse. *Nature*, **358**, 369-370.

Sud, Y. C., G. K. Walker, and K.-M. Lau, 1999: Mechanisms regulating sea-surface temperatures and deep convection in the tropics. *Geophys. Res. Latters*, **26**, 1019-1022.

Waliser, D. E., and N. E. Graham, 1993: Convective cloud systems and warm-pool sea surface temperatures: Coupled interactions and self-regulation. *J. Geophys. Res.*, **98**, 12881-12893.

Wallace, J. M., 1992: Effect of deep convection on the regulation of tropical sea surface temperature. *Nature*, **357**, 230-231.

Wentz, F. J., 1997: A well calibrated ocean algorithm for SSM/I. *J. Geophys. Res.*, **102**, 8703-8718.

Figure Captions

Figure 1. Distributions of the sea surface temperature (a), high-level cloud cover (b), and wind speed (c) in the tropical western Pacific and eastern Indian Ocean averaged over a three-year (1998-2000) period.

Figure 2. Distributions of the surface solar heating (a), evaporative cooling (b), and the total heating (c) in the tropical western Pacific and eastern Indian Ocean averaged over a three-year (1998-2000) period.

Figure 3. Monthly-mean SST, the insolation at the top of the atmosphere, S_o, the surface solar heating, SW, and the evaporative cooling, LH, averaged over the domain 5° N-15° N and 130° E-160° E. Units are ° C for SST and W m^{-2} for heat fluxes.

Figure 4. Same as Fig. 1, except for the difference between the months of December, January, February (DJF) and the months of June, July, August (JJA).

Figure 5. Same as Fig. 2, except for the difference between the months of December, January, February (DJF) and the months of June, July, August (JJA).

Figure 6. Same as Fig. 1, except for the difference between December-February 1997-1998 (El Nino) and December-February 1998-1999 (La Nina).

Figure 7. Same as Fig. 2, except for the difference between December-February 1997-1998 (El Nino) and December-February 1998-1999 (La Nina).

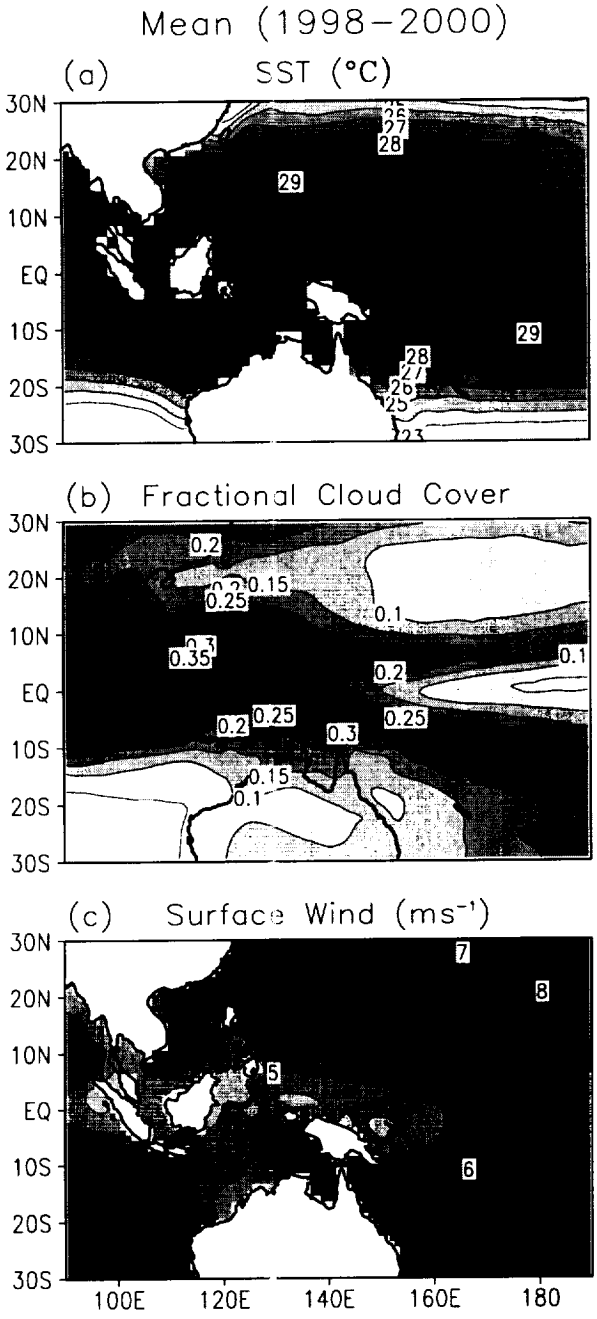
Mean (1998–2000)
(a) SST (°C)
30N
20N
10N
EQ
10S
20S
30S
29
28
29
(b) Fractional Cloud Cover
0.2
0.15
0.25
0.1
0.35
0.2
0.1
0.2
0.25
0.3
0.25
0.15
0.1
(c) Surface Wind (ms⁻¹)
7
8
5
6
100E
120E
140E
160E
180

Fig 1

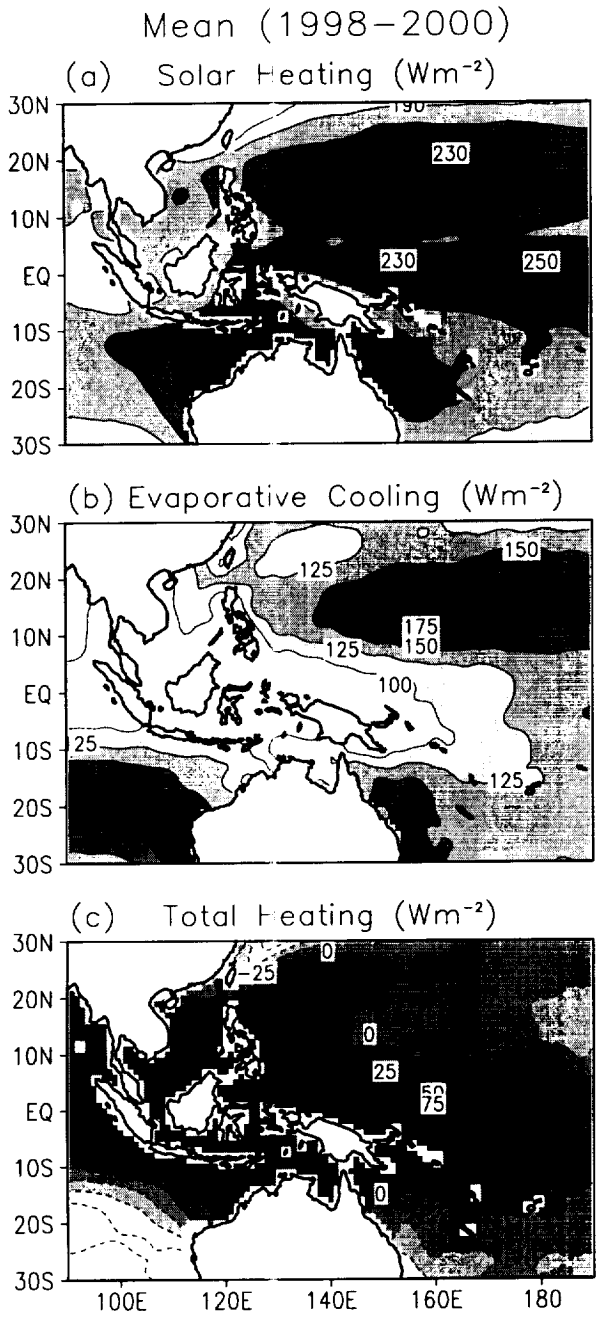
Mean (1998–2000)
(a) Solar Heating (Wm⁻²)
30N
20N
10N
EQ
10S
20S
30S
230
230
250
(b) Evaporative Cooling (Wm⁻²)
150
125
175
150
125
100
25
125
(c) Total Heating (Wm⁻²)
0
-25
0
25
75
0
100E
120E
140E
160E
180

fig 2

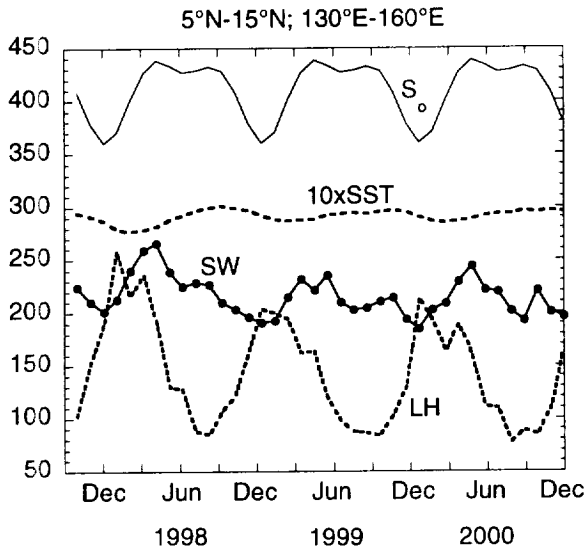

Figure 3 (Area 9)

F.g.3

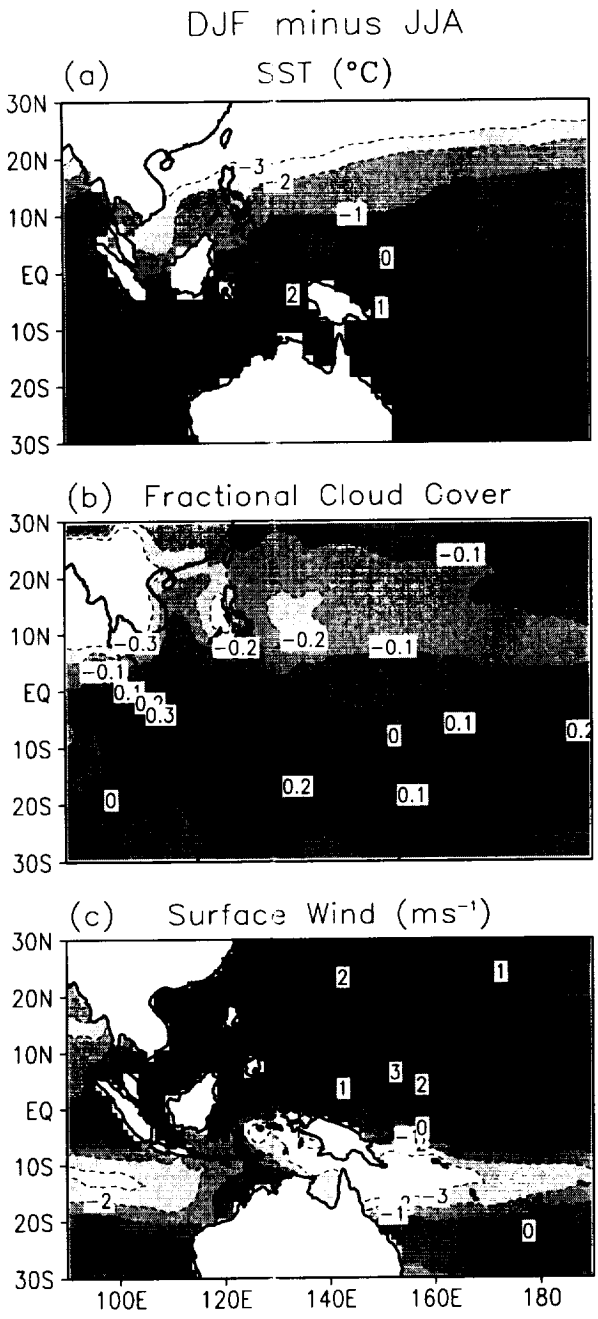
DJF minus JJA
(a) SST (°C)
30N
20N
10N
EQ
10S
20S
30S
(b) Fractional Cloud Cover
(c) Surface Wind (ms⁻¹)
100E
120E
140E
160E
180

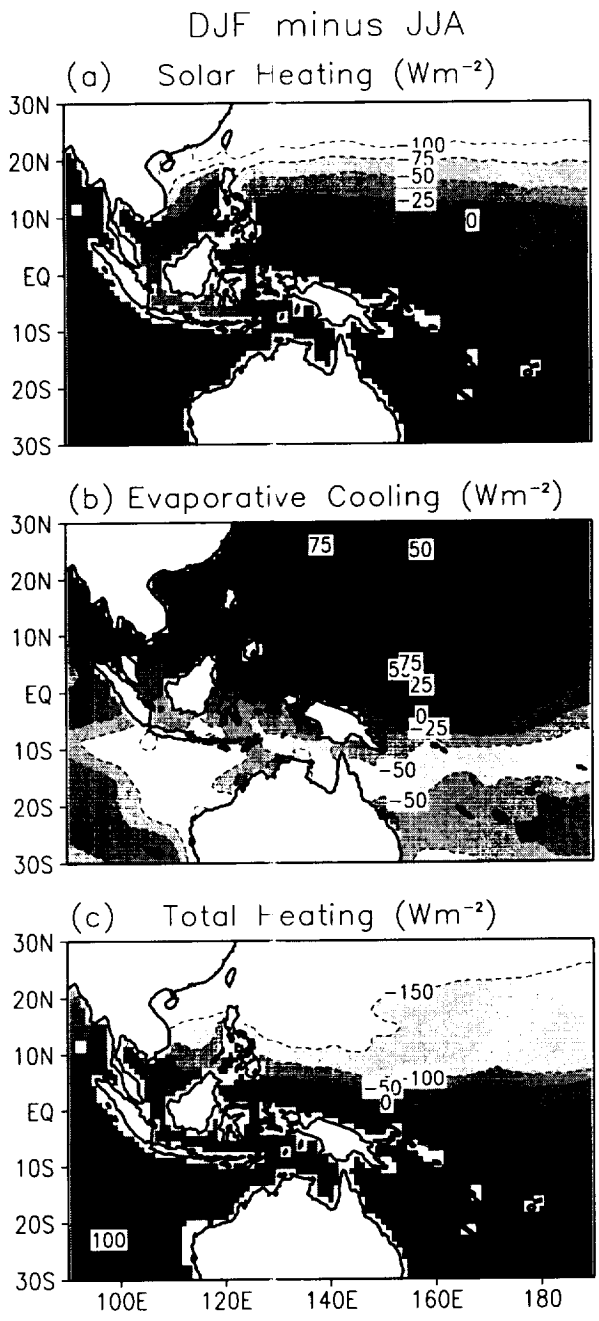
DJF minus JJA
(a) Solar Heating (Wm⁻²)
30N
20N
10N
EQ
10S
20S
30S
100
75
50
25
0
(b) Evaporative Cooling (Wm⁻²)
75
50
75
25
0
25
50
50
(c) Total Heating (Wm⁻²)
150
100
50
0
100
100E
120E
140E
160E
180

Fig 5

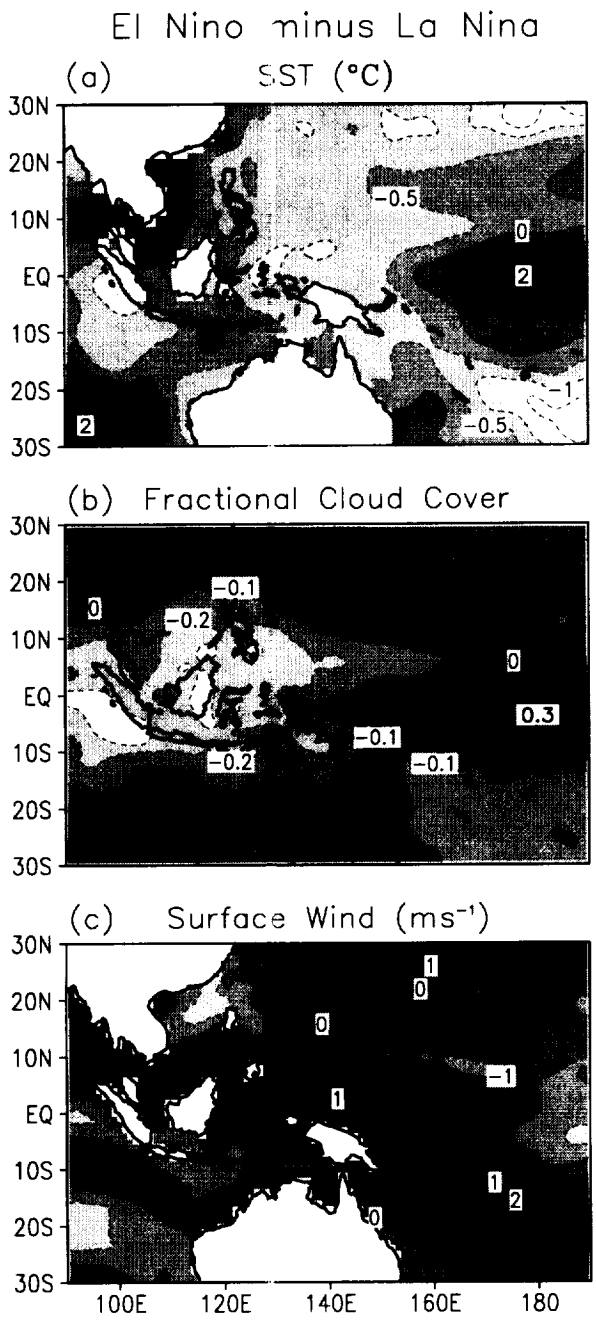
El Nino minus La Nina
(a) SST (°C)
30N
20N
10N
EQ
10S
20S
30S
−0.5
0
2
−1
−0.5
2
(b) Fractional Cloud Cover
−0.1
0
−0.2
0
0.3
−0.1
−0.2
−0.1
(c) Surface Wind (ms⁻¹)
1
0
0
−1
1
1
2
0
100E
120E
140E
160E
180

fig 6.

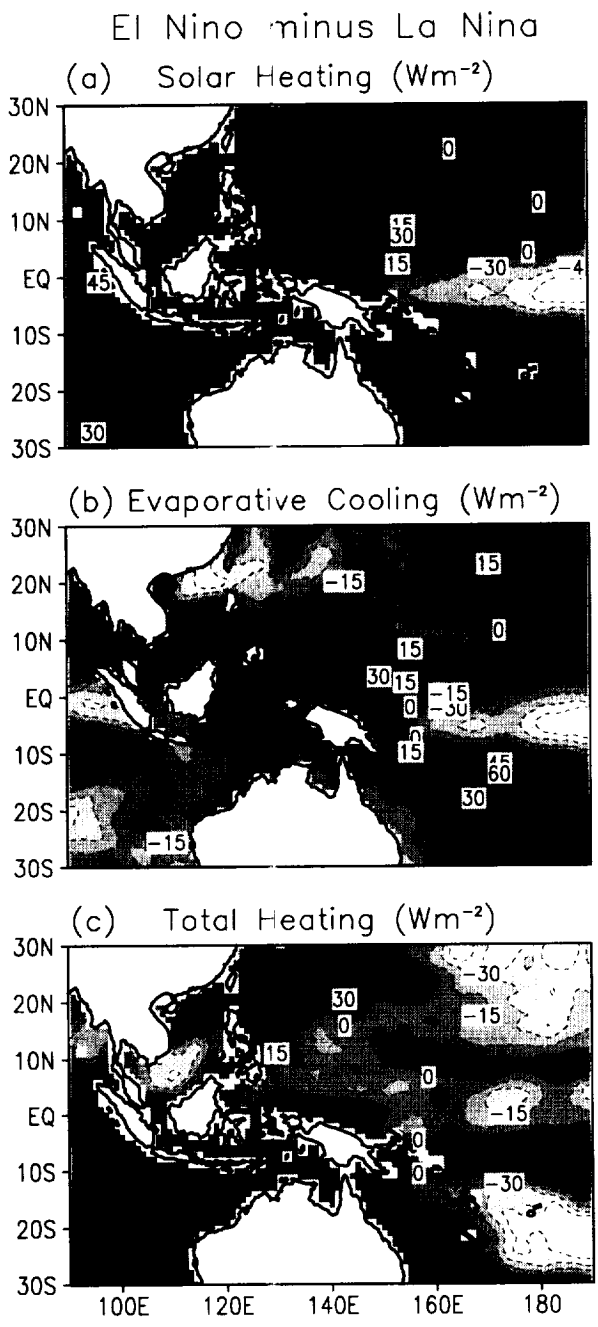
El Nino minus La Nina
(a) Solar Heating (Wm⁻²)
30N
20N
10N
EQ
10S
20S
30S
0
0
15
30
15
0
-30
-4
45
30
(b) Evaporative Cooling (Wm⁻²)
-15
15
0
15
30
15
-15
0
-30
0
15
45
60
30
-15
(c) Total Heating (Wm⁻²)
-30
30
0
-15
15
0
-15
0
0
-30
100E
120E
140E
160E
180